Effect of ultrasonic nanocrystal surface modification on the characteristics of AISI 310 stainless steel up to very high cycle fatigue

Khan, M. K. , Liu, Y.J. , Wang, Q.Y. , Pyun, Y.S. and Kayumov, R.

Effect of Ultrasonic Nanocrystal Surface Modification on the Characteristics of AISI 310 Stainless Steel up to Very High Cycle Fatigue

M. K. Khan[1,3*], Y. J. Liu[1], Q. Y. Wang[1], Y. S. Pyoun[2], R. Kamyrouv[2]

[1] *Department of Mechanics and Engineering Science, Sichuan University, Chengdu, 610065, China*

[2] *Department of Mechanical Engineering, Sun Moon University, Asan-si, 336-708, Chungnam, South Korea.*

[3] *Department of Mechanical Engineering, DHA Suffa University, Karachi, 75500, Pakistan.*

Email: kashooo@engineer.com*

Abstract

Effects of Ultrasonic Nanocrystal Surface Modification (UNSM) on the very high cycle fatigue response of AISI 310 stainless steel have been investigated. The higher impact force used in UNSM treatment showed a higher fatigue life improvement. The fatigue life improvement was higher in crack initiation from the surface of specimens. The subsurface crack initiation depth in the alloy increased with increase in the fatigue failure cycles. It was concluded that UNSM treatment can increase the life of the alloy significantly up to very high cycle fatigue.

Keywords Ultrasonic Nanocrystal Surface Modification, Very High Cycle Fatigue, Crack Initiation, Subsurface Cracks, Surface Hardness

Nomenclature

N_f	Number of Failure Cycles
K_f	Fatigue Life Improvement Factor
R_a	Surface Roughness
a_{FGA}	Size of Fine Granular Area
ΔK_{th}	Stress Intensity Factor

1. Introduction

Fatigue cracking is the most common damage mechanism in materials and structures under dynamic loading. The fatigue cracks initiate from the stress concentration regions and may limit the service life significantly. In many cases, the aerospace, automotive, locomotive and wind energy structures are expected to serve a fatigue life more than 10^7 cycles. Hence, improvement of the fatigue life up to 10^9 to 10^{10} cycles is gaining continuous attraction of researchers. The use of mechanical work to transfer energy in the materials for improvement of the surface properties and fatigue life has been proved very successful in the past [1-4]. The techniques like Laser Shock Peening (LSP), Shot Peening (SP), Ultrasonic Shot Peening (USP) and Ultrasonic Nanocrystal Surface Modification (UNSM) have shown substantial effectiveness in improvement of the fatigue life [3-5]. These techniques plastically deform the material surface and produce compressive residual stresses up to a significant depth. However, most studies have focused on the fatigue life improvement up to 10^7 fatigue cycles only and studies about the effectiveness of surface treatment process in improvement of the fatigue life at very low stresses up to very high fatigue cycles are very limited [6].

The formation of nanostructure layer on the material surface in the surface treatment is very effective in delaying the fatigue crack initiation. The fatigue life improvement depends on the plastic deformation and elastic residual stresses developed in the formation of nanostructure layer on the material [3-4]. These parameters depend on the elastic-plastic properties of the target material and process parameters used in the treatment. The higher fatigue life improvement is achieved when optimum plastic deformation, surface roughness and the compressive residual stress fields are developed. However, there is no such model which takes into account all these parameters to explain the fatigue life improvement in alloys. Hence, case by case experimental investigations are carried out to investigate the effect of surface treatment on the improvement of fatigue life of alloys.

In fatigue loading, the cracks initiate from surface or sub-surface of the material depending on the applied stresses and fatigue cycles to failure. The fatigue cracks initiate from the surface of specimens up to 10^7

cycles and beyond that the subsurface crack initiation is observed. However, there are many alloys in which the fatigue cracks always initiate from the surface of material even beyond 10^7 cycles. The surface treatment of these alloys show subsurface crack initiation beyond 10^7 cycles. Therefore, the mechanism of subsurface cracking in these alloys is observed only due to the surface treatment.

The Ultrasonic Nanocrystal Surface Modification (UNSM) is a surface treatment technique which shows a higher fatigue life improvement and wear rate in the alloys as compared to the conventional shot peening, laser shock peening and other techniques [1, 4, 7, 9]. In the UNSM process, the material is targeted by striking ultrasonically to convert the microstructure into nanocrystals up to a certain depth. This produces a compressive residual stress field in the material which can go as deep as 500μm into the surface. The plastic deformation and compressive residual stresses help in delaying the fatigue crack initiation and improving the fatigue life of the material [7-9].

The UNSM has been applied by some researchers on various engineering alloys for improvement in wear and fatigue properties. Pyoun et al. [1] applied UNSM on different engineering alloys and improved the surface roughness and fatigue properties. Cao et al. [2] on S45C steel, Wu et al. [4] on plasma nitride S45C steel and Suh et al. [8-9] on SKD-61 steel, used UNSM and improved the fatigue strength of the alloys significantly. Cherif et al. [7] on stainless steel alloys while Amanov et al. [10] on AZ91D magnesium alloy, used UNSM and improved the wear rate up to 30%. Zhou et al. [11] found that the UNSM application on SMAT steel sample produce a relatively thicker refined layer than on pure Fe. It has been found in these studies that the fatigue life improvement by UNSM was a complex interaction of the elastic-plastic properties of the target material and its microstructure. The UNSM process parameters like diameter of the striking tip, impact force of striking, and the feed rate were also found to be important for improvement of fatigue life [2]. The better fatigue life improvement was obtained when optimum process parameters based on the elastic-plastic properties were used [2-4]. However, up to now most of the development in fatigue life improvement is empirical and there is no model which can explain the fatigue life improvement mechanism in surface and subsurface crack initiation.

In this study, the UNSM was used to improve the fatigue life of AISI 310 stainless steel. Two different impact forces and feed rates were used in the treatment. The S-N curve of the material showed a substantial improvement in the fatigue life in all specimens. The alloy showed surface cracking up to 10^9 cycles before the UNSM treatment [12-13]. However, the UNSM treated specimens showed subsurface cracking beyond 10^7 cycles. The crack initiation site reached to as deep as 800 µm below the surface. The UNSM treatment increased the hardness of the alloy by 15%. It was concluded that suitably chosen UNSM process parameters can increase the fatigue life up to VHCF.

2. Materials & experimental details

In this study, cylindrical rods of 12 mm diameter AISI 310 were used. The alloy is frequently used in heat exchangers, pipes and machinery parts due to its excellent combination of strength, corrosion resistance, weld and machinability. Elastic–plastic properties of the material are given in Table 1. Metallographic samples were prepared up to 0.05 µm finish. Diluted Aqua Regia Reagent for 120 sec was used for etching the samples. The grain size of the material was found to be ~10 µm as shown in Fig. 1. The grains were equiaxed and found to have a random orientation. Carbide precipitates were obtained on the grain boundaries of the material [12-13].

Vickers micro hardness tester was used on the cross section of the specimens after UNSM treatment. The indentations were made at 50 mN load from the subsurface of the specimen with a spacing of 25 to 30um. The hardness testing was carried out at three different locations in each specimen to avoid any scatter in the data.

The ultrasonic fatigue testing was carried out at a load ratio R = -1 up to very high cycle fatigue (VHCF) range. The fatigue samples were designed to resonate longitudinally at 20 kHz with the ultrasonic fatigue testing system. Compressed air was used for cooling of specimens to avoid excessive heating in the ultrasonic fatigue testing. The specimen geometry used in the VHCF testing is shown in Fig. 2. The

surface of the specimens was polished to surface roughness R_a $0.2\,\mu m$. Surface roughness of the specimens was measured with Atomic Force Microscope (AFM) and found to be ~80 nm.

In the UNSM process, an ultrasonic generator and air compressor are used to strike the material with a tungsten carbide ball at 30µm amplitude and ultrasonic frequency of 20 kHz. The ball strikes the material with a contact pressure of 3-30GPa and excitation of 1000 to 100,000 strikes/mm². The ball strikes a particular area of the specimen and then uses a feed rate for horizontal displacement and target again the material. Hence, a lower feed rate is used for a larger overlapping of the impact regions. Fig. 3(a) shows the process set-up of UNSM and Fig. 3 (b) shows the schematic representation of the microstructure of alloy due to UNSM treatment [1-3].

In this study, a 2.4mm diameter ball was used for striking the material. The static impact force of 20 and 30N was used, each with feed rate of 0.04 and 0.07 mm/rev. In UNSM treatment, a coolant was continuously used on the specimens to avoid excessive heating. Fig. 4 (a) shows the surface profile of the specimen after UNSM treatment from an optical microscope. The UNSM processing marks were found on the specimen surface. The specimens showed better surface roughness after UNSM treatment [14]. Fig. 4 (b) shows the effect of UNSM on the cross-section of the specimen. Microstructure of the specimen inside the circular line was found to be different near the surface of specimen. The specimens showed a refined grain layer at the edges of the cross-section. High density dislocations with several nanograins were observed near the surface of specimen. The specimens treated with 30N impact force showed a deeper and more refined nanostructured layer. The refined layer depth was found to be 120 and 80µm in 30 and 20N impact force treated specimens, respectively.

Tensile properties of specimens after UNSM were investigated and it was found that there was no evident effect of UNSM treatment on the elastic-plastic properties of the material. This may be attributed to the fact that effect of UNSM treatment was up to only ~300µm in the sample surface.

3. Results and Discussions

3.1- S-N Curves

3.1.2 AISI 310

Fig. 5 shows the S–N curve of the alloy before and after the UNSM treatment with 20 and 30N impact force each at 0.04 and 0.07 mm/rev feed rate. The S-N curve before treatment showed a decreasing slope up to 10^7 cycles. The material showed a fatigue limit at 500MPa. A semi-asymptote type curve was obtained. The failure cycles of alloy increased substantially at lower stresses. This showed that the fatigue cracking at relatively lower stress levels in the alloy consumed higher fatigue cycles.

The S-N curve of the UNSM treated specimens showed significant improvement in the fatigue life. The fatigue life of the specimens treated with 30N impact force was found to be substantially higher than those treated with 20N impact force [15]. The effect of UNSM treatment was found to be different in entire S-N curve. The fatigue strength improvement was higher in specimens failed up to 10^7 cycles than those failed beyond 10^7 cycles.

3.2- Fractography

The fatigue crack initiation sites and fracture surfaces were investigated using Scanning Electron Microscope (SEM). Fig. 6 shows the fracture surface of an untreated specimen failed at 550MPa. The specimens without UNSM treatment showed crack initiation from the surface of the specimens at all failure cycles. The fish-eye or subsurface crack initiation was not observed. The fracture surface showed high density radial lines, ridges and zones with many secondary cracks and pores in the subsurface. Cleavage fracture was observed all along the surface of the specimen. The specimens failed at lower fatigue cycles showed fewer radial ridges than those failed at higher fatigue cycles. This was attributed to the local plasticity accumulation at the surface of specimens loaded at the lower stress levels. More details of the fracture surfaces and crack initiation in the specimens can be seen elsewhere [12-13].

The specimens with UNSM treatment found to have different fracture mechanisms. Up to 10^7 cycles, the cracks initiated from the surface of specimen. Fig. 7 shows the fracture surface of a specimen failed at

less than 10^7 fatigue cycles. The fracture surface showed a "canyon" type fracture with a sidestep between two crack propagation regions on two different planes. In some specimens, multiple crack initiation sites were observed similar to the untreated specimens failed at higher stresses. The crack initiation from specimen surface was attributed to the surface defects and carbide precipitations [12].

The UNSM treated specimens, failed beyond 10^7 cycles, showed a subsurface crack initiation. The cracks were found to be initiated from local inclusions in the subsurface as shown in Fig. 8. The fracture of specimens showed no difference with variation in the treatment impact force and feed rate. The crack initiation was found to have a "fish-eye" in agreement with earlier studies [16-19]. The fracture surface showed an inclusion, a small dark area and a large circular area. The small dark area with inclusion at its center was observed. The area, also known as Fine Granular Area (FGA), and the fish eye were surrounded by another larger circular area. The composition of inclusion was found to be different than that of bulk material [16-17]. The subsurface crack initiation depth was found to be different in the specimens.

Fig. 9 shows the detailed view of an inclusion and its associated FGA region. The FGA found to have granular morphology and higher roughness in the fracture surface [18-19]. The higher roughness of the FGA may be attributed to the higher fatigue cycles. At the end of "penny-shaped" FGA zone, high proportion large radial ridges were observed with fish-eye inclusion as the geometric center [17, 20-21]. The composition of inclusion was measured by EDS (Electric dispersive spectroscopy) which was found to be Al, Ti, Mg and other materials. The inclusion which served as a crack initiation site was attributed to a metallurgical heterogeneity, supergrain or pore [17].

Fig. 10 shows the 3D scan from laser scanning microscope of a 25μm x 25μm region inside FGA. The surface of FGA was found to be extremely rough with multiple crusts and troughs. The height and depth of each feature of FGA was measured and found to be around 1μm as observed in earlier studies [19-21]. This was attributed to the local plasticity accumulation in the FGA due to the fatigue cycling and stress concentration [17].

In some specimens, a distinct FGA region around inclusion was not observed [17]. Fig. 11 shows a magnifying image of an inclusion in a specimen treated with 30N impact force with 0.04 mm/rev feed rate. The size of inclusion in the absence of FGA was relatively larger. The surface found to have multiple arrested cracks around the inclusion. This showed that the crack initiation from an inclusion with or without FGA required a sufficient size of the region with accumulated plasticity.

3.3- Hardness Analysis

Fig. 12 (a) and (b) show the effect of UNSM treatment on the hardness of the specimens' cross-section. The dashed line shows the bulk hardness of the alloy before treatment. The hardness of specimens was 15% higher at the surface which continuously decreased with increase in the subsurface distance [1-4]. The hardening effect was observed up to a certain depth in all specimens.

It was found that all treatment parameters increased the surface hardness of the samples. The depth of hardening was greater for 30N impact force treated specimens. The effect of hardening was found up to 250μm in 20N impact force treated specimens. However, for 30N impact force treated specimens the hardening was found to be up to 300μm. This may be attributed to a deeper nanocrystal depth in specimens treated with higher impact force [4, 10, 14]. The higher force used in treatment produced a deeper nanocrystal layer with relatively smaller grain size and increased the hardening depth [3]. Similarly, a stronger and deeper hardening depth was observed for lower feed rate. The lower feed rate led to a higher overlapping of the impact region during treatment resulted in higher hardness.

3.4 Residual Stresses

X-rays diffraction was used to measure the surface residual stresses in the specimens. Table 2 shows the residual stress components on the surface of specimens. The specimens treated with higher force found to have relatively higher compressive residuals stresses [2, 4]. The longitudinal component of stress was found to be different than the transverse component. It can be said that the higher impact force increased

the elastic residual stresses and plastic deformation of material. However, in a separate study on the same alloy, 40 and 60N impact force was also used. It was found that further increase in impact force decreased the hardening of material surface without changing the residual stresses. This may be attributed to the work hardening capability of material which showed increase in hardness with impact force to a certain extent and further increase in impact force showed no further effect on hardness of material.

The effect of loading cycles on relaxation of residual stresses was also investigated. Few samples were fatigue loaded up to 10^3 cycles. The residual stresses were found to be similar before and after fatigue testing. This showed that there was no effect of loading cycles on the residual stress relaxation.

3.5 Crack Initiation

The fatigue loading of specimens before UNSM treatment showed crack initiation from the surface of specimens. In our earlier study, the mechanism of crack initiation was found to be different up to 10^9 cycles [12-13]. The specimens failed up to 10^7 cycles showed a damage free surface without slip markings, and the cracks initiation was found from the surface defects and carbide precipitates. The crack initiation was observed from high density PSBs and deformations for specimens failed beyond 10^7 cycles. The AFM scanned image of the specimen surface showed wide and broad PSBs. The surface showed several intrusions and extrusions with very small separation distance. It was concluded that the fatigue cracks initiated from the deepest intrusion owing to the highest stress concentration around its sharp edges. The shallow cracks nucleated from these slip markings or other nearby heterogeneities and defects. More details of the crack initiation from PSBs can be found elsewhere [12].

In the UNSM treated specimens, the fracture surface showed different crack initiation regions. The specimens failed up to 10^7 cycles showed surface crack initiation from the surface defects and carbide precipitations as observed in previous studies of untreated specimens [12-13]. However, the specimens failed beyond 10^7 cycles showed a subsurface crack initiation. Fig. 13 shows the crack initiation depth of UNSM treated specimens failed at different fatigue cycles [22]. The crack initiation depth increased with increase in the fatigue cycles. The minimum crack initiation depth was 300µm in all type of specimens.

This was in agreement with surface hardness profiles of UNSM treated specimens where the hardening effect up to 250 to 300μm below the surface was present. This showed that the surface hardening in the region up to 300μm stopped the crack initiation from this region. The slope of increasing crack initiation depth with fatigue cycles was higher in specimens treated with 30N impact force. The specimens treated with 20N force showed subsurface crack initiation depth as 350 to 450μm. However, the depth was 300 to 850μm in specimens treated with 30N force. The higher crack initiation depth in 30N impact force treated specimens was due to deeper hardening depth and higher compressive stresses [2, 4]. At lower stresses, a higher fatigue cycles were required to initiate the cracks. In addition, the cracks initiated from the regions with lower hardening and compressive residual stresses. The specimens treated with 20N impact force showed crack initiation from the subsurface region near the hardened regions. In 30N impact force treated specimens, the hardened layer was deeper hence the crack initiation was observed from a deeper subsurface location. The increase in fatigue life with crack initiation depth led to a conclusion that deeper inclusions were more prone to crack initiation at lower stresses [20].

For specimens with subsurface crack initiation, the areas of FGA (a_{FGA}) was measured with image analysis software Image-J. The corresponding stress intensity factor ΔK_{th} for a_{FGA} was calculated based on the Murakami's model [18]. Fig. 14 shows the variation of ΔK_{th} with the fatigue cycles for different UNSM treated specimens failed beyond 10^7 fatigue cycles. The ΔK_{th} was constant with variation in the fatigue cycles and UNSM process parameters [19-20, 22]. The ΔK_{th} values were found to be 4 to 5 MPa$\sqrt{m}$, roughly corresponding to the stress intensity factor range of the alloy AISI 310. It can be concluded that when the ΔK_{th} value reach to the critical size, the specimen fail catastrophically. In the absence of FGA, the cracks initiate from the inclusion and a larger inclusion size is observed [17]. However, a similar ΔK_{th} value is obtained for inclusions with or without FGA.

It can be said that the FGA surface with a higher surface roughness is due to the plasticity accumulation around the inclusion in the fatigue loading. This process debonds material in the inclusion vicinity and form a FGA [20-21]. The required number of fatigue cycles for debonding the material and extending the

size of FGA depends on the microstructure and strength of the grain boundaries in the region. The local plasticity accumulated regions coalescence together to form a rough surface [20]. When the ΔK_{th} of the FGA reaches to a threshold value $4-5 MPa\sqrt{m}$, the cracks start to propagate. At lower stresses, a higher fatigue cycles are required to achieve ΔK_{th} value $4-5 MPa\sqrt{m}$. Hence, it can be concluded that the formation of a FGA around inclusion or a large size inclusion without FGA dictates the fatigue life of the specimens [17].

Furthermore, it can be said that the UNSM delays the local plasticity accumulation around the inclusions by hardening of the specimen surface and producing compressive residual stresses. The material surface is subjected to a severe plastic deformation by refining of grains, increasing number of grain boundaries and producing high density dislocations. In specimens treated with a higher impact force, a relatively deeper hardening depth and residual stresses in combination promote the crack initiation from higher depths and subsequently increase the fatigue life [2, 4].

3.6 Fatigue Life Improvement

The fatigue life improvement from UNSM treatment can be divided into surface and subsurface crack initiation. Fig. 15 shows the fatigue life improvement factor 'K_f' variation with failure cycles for all type of UNSM treatment specimens. The 'K_f' was obtained as the ratio of fatigue life with and without UNSM treatment ($K_f = N_{UNSM}/N_{Without\ UNSM}$). The variation in K_f with fatigue failure cycles was substantial before and beyond 10^7 fatigue cycles. The K_f increased with increase in the fatigue failure cycles up to 10^7 cycles. The highest K_f was observed at 10^7 cycles. For specimens treated with 20N impact force, the K_f was found to be 20 at 10^7 fatigue cycles. In specimen treated with 30N impact force a higher fatigue life was observed up to 10^7 cycles. The K_f in these specimens was found to be 40 at 10^7 cycles.

The crack initiation was observed from the subsurface of specimen beyond 10^7 fatigue cycles. The fatigue life improvement factor found to be decreased sharply with further increase in the fatigue failure cycles. This showed that shift in crack initiation to the subsurface of the material decreased the fatigue life

improvement. This led to a fatigue life similar to those of untreated specimens at 10^9 fatigue cycles. However, the specimens treated with 30N impact force showed a significantly higher K_f than those treated with 20N impact force. The 30N impact force treated specimens found to have higher fatigue life improvement beyond 10^7 cycles as well.

The role of residual stress field is very important in surface treatment based fatigue life improvement. In surface cracking phenomenon, knowledge of surface compressive residual stresses may be enough. The surface treatment phenomenon generates compressive residual stresses in the surface of material up to 200 to 300μm and to maintain the equilibrium state of the specimen; compensatory tensile residual stresses develop in the subsurface of the specimen [1, 3, 8]. These tensile residual stresses may promote the subsurface fatigue cracking [5]. Hence, the full field residual stress determination is very important especially in the subsurface cracking phenomenon. It can be said that in VHCF those residual stress fields are beneficial in which the balancing tensile residual stresses are minimum. The measurement of through thickness residual stresses up to higher depths in the alloys is challenging. The residual stress profiles and their role in improvement of the fatigue life up to very high cycles will be reported in future. In addition, the hardening depth and microstructure produce in treatment are also very critical in improvement of the fatigue life. It can be concluded that the fatigue life improvement up to very high cycles is a complex interaction of the UNSM process parameters, microstructure, elastic-plastic properties of the material, and residual stresses developed in the process. The surface and subsurface crack initiation transition make the understanding of crack initiation mechanism more challenging.

4- Conclusions

The fatigue characteristics of AISI 310 stainless steel after UNSM treatment have been investigated up to very high loading cycles. It was found that the fatigue life improvement up to very high cycles was a function of the UNSM process parameters, microstructure, elastic-plastic properties of the material, and residual stresses developed in the process. The higher fatigue life improvement was obtained in

specimens with crack initiation from the surface of material. The subsurface crack initiation depth in the alloy increased substantially with increase in the fatigue cycles. It was concluded that the optimized UNSM process parameters may increase the fatigue life of the alloy substantially up to very high loading cycles.

5- Acknowledgements

5- References

[1] Pyoun, Y. S., and Kayumov, R. (2012) The concepts and properties of nano-skin materials and components created by ultrasonic nanocrsytal surface modification. Adv. Mat. Dev. Perf., 6 527-533.

[2] Cao, X. J., Pyoun, Y. S., and Murakami, R. (2010) Fatigue properties of a S45C steel subjected to ultrasonic nanocrystalsurface modification. App. Surf. Sci., 256, 6297–6303.

[3] Suh, M. S., Suh, C. M, and Pyoun, Y. S. (2013) Very high cycle fatigue characteristics of a chrome-molybdenum steel treated by ultrasonic nanocrystal surface modification technique. Fatigue Fract. Eng. Mater. Struct., 36, 769–778.

[4] Wu, B., and Wang, P. (2012) Effect of ultrasonic nanocrystal surface modification on the fatigue behaviors of plasma-nitrided S45C steel. Surf. Coat. Tech., 213, 271–277.

[5] Dorman, M., and Toparli, M. B. (2012) Effect of laser shock peening on residual stress and fatigue life of clad 2024 aluminium sheet containing scribe defects. Mat. Sci. Eng. A., 548, 142–151.

[6] Trsko, L., Bokuvka, O., Novy, F., and Guagliano, M. (2014) Effect of severe shot peening of ultra-high-cycle fatigue of low-alloy steel. Mat. Des., 2014, 103-113.

[7] Cherif, A., Pyoun, Y. S., and Scholtes, B. (2010) Effects of Ultrasonic Nanocrystal Surface Modification (UNSM) on Residual Stress State and Fatigue Strength of AISI 304. J. Mat. Eng. Perf., 19,

282-286.

[8] Suh, C. M., Song, G. H., Suh, M. S., and Pyoun Y. S. (2007) Fatigue and mechanical characteristics of nano-structured tool steel by ultrasonic cold forging technology. Mat. Sci. Eng. A., 443, 101–106.

[9] Suh, C. M., Lee, M. H., and Pyoun Y. S. (2010) Fatigue characteristics of skd-61 by ultrasonic nanocrystal surface modification technology under static load variation. Int. J. Mod. Phy. B., 24, 2512-2517.

[10] Amanov, A., Penkov, O. V., and Pyoun, Y. S. (2012) Effects of ultrasonic nanocrystalline surface modification on the tribological properties of AZ91D magnesium alloy. Trib. Int., 54, 106-113.

[11] Zhou, L., Liu, G., Ma, X. L., and Lu, K. (2008) Strain-induced refinement in a steel with spheroidal cementite subjected to surface mechanical attrition treatment. Act. Mat., 56, 78-87.

[12] Khan, M. K., and Wang, Q. Y. (2013) Investigation of crack initiation and propagation behavior of AISI 310 stainless steel up to very high cycle fatigue. Int. J. Fat., 54, 38–46.

[13] Khan, M. K., Liu, Y. J., Wang, Q. Y., and Pyoun, Y. S. (2015) Effect of small scale notches on the very high cycle fatigue of AISI 310 stainless steel. Fatigue Fract. Eng. Mat. Struct., 38, 290-299.

[14] Amanov, A., Cho, I. S., Pyoun, Y. S., Leeb, C. S., and Park I. G. (2012) Micro-dimpled surface by ultrasonic nanocrystal surface modification and its tribological effects. Wear., 286, 136– 144.

[15] Zhang, K. Y., Pyoun, Y. S., Cao, X. J., Wu, B., and Murakami, R. (2012) Fatigue properties of SUS304 stainless steel after ultrasonic nanocrystal surface modification (UNSM). Adv. Mat. Dev. Perf., 6, 330-335.

[16] Wang, Q. Y., Bathias, C., Kawagoishi, N., and Chen, Q. (2002) Effect of inclusion on subsurface crack initiation and gigacycle fatigue strength. Int. J. Fat., 24, 1269–1274.

[17] Huang, Z., Wagner, D., Bathias, C., and Paris, P. (2010) Subsurface crack initiation and propagation mechanisms in gigacycle fatigue. Act. Mat., 58, 6046–6054.

[18] Murakami, Y., Nomoto, T., and Ueda, T. (1999) Factors influencing the mechanism of superlong fatigue failure in steels. Fatigue Fract. Eng. Mat. Struct., 22, 581–590.

[19] Shiozawa, K., Mori, Y., Nishino, S., and Lu, L. (2006) Subsurface crack initiation and propagation mechanism in high-strength steel in a very high cycle fatigue regime. Int. J. Fat., 28, 1521–1532.

[20] Sakai, T., Sato, Y., and Oguma, N. (2002) Characteristic S-N properties of high-carbon-chromium-bearing steel under axial loading in long-life fatigue. Fatigue Fract. Eng. Mat. Struct., 25, 765-773.

[21] Sakai, T., Sato, Y., Nagano, Y., Takeda, M., and Oguma, N. (2006) Effect of stress ratio on long life fatigue behavior of high carbon chromium bearing steel under axial loading. Int. J. Fat., 28, 1547–1554.

[22] Shiozawa, K., Lu, L., and Ishihara, S. (2001) S–N curve characteristics and subsurface crack initiation behaviour in ultra-long life fatigue of a high carbon-chromium bearing steel. Fatigue Fract. Eng. Mat. Struct., 24, 781–790.
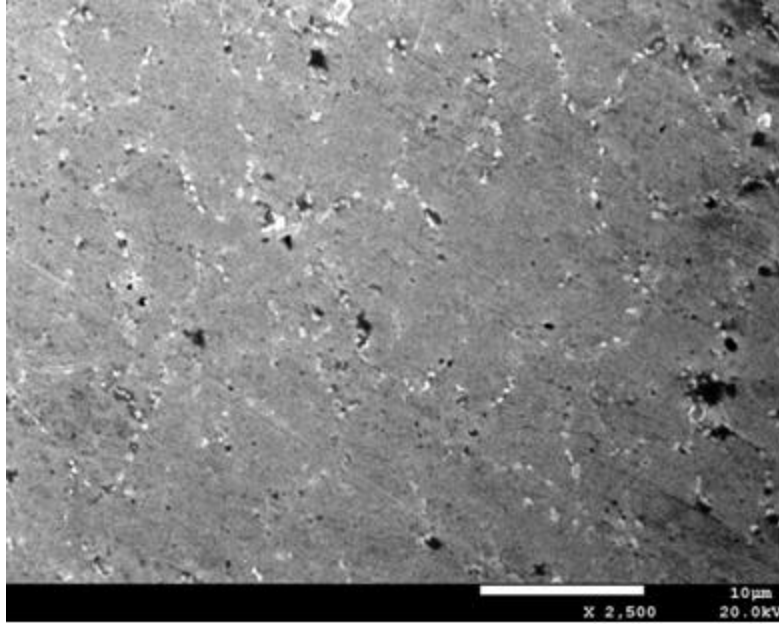
Fig. 1-SEM micrograph shows carbide precipitates at grain boundaries.
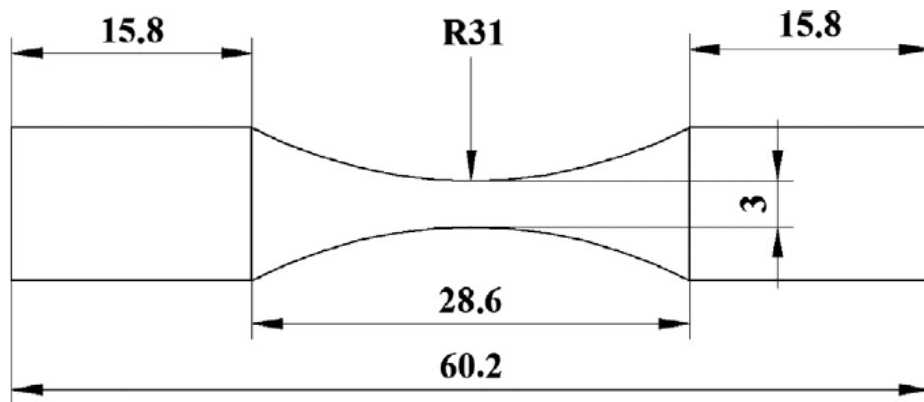
Fig. 2- Schematic representation of fatigue specimen

(a)

Micro-dimples

10μm
30μm
100μm
~50 nm grain
~100 nm grain
~500 nm grain

Original grain size ~1500nm

Compressive stress/strain structure

(b)
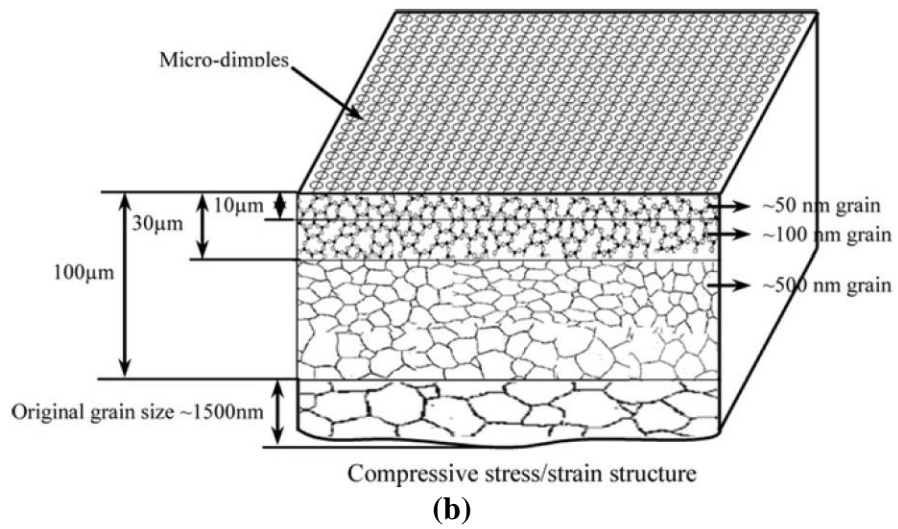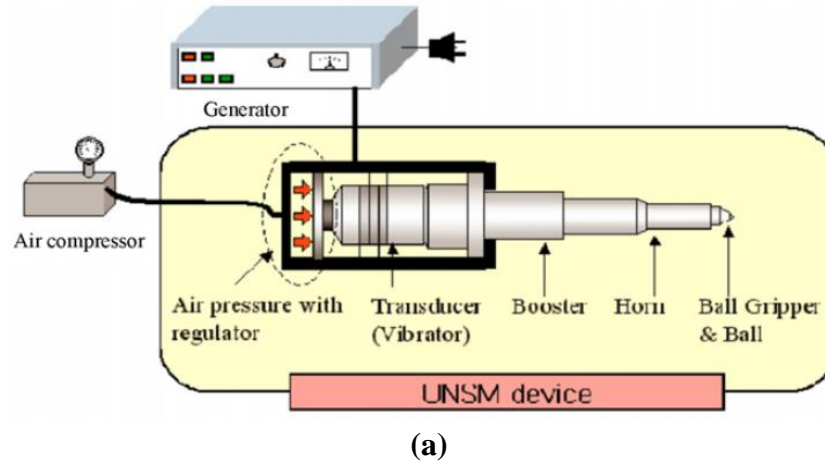
Fig. 3- (a) UNSM process set-up (b) Schematic representation of the effect of UNSM on microstructure of the material [1-3]
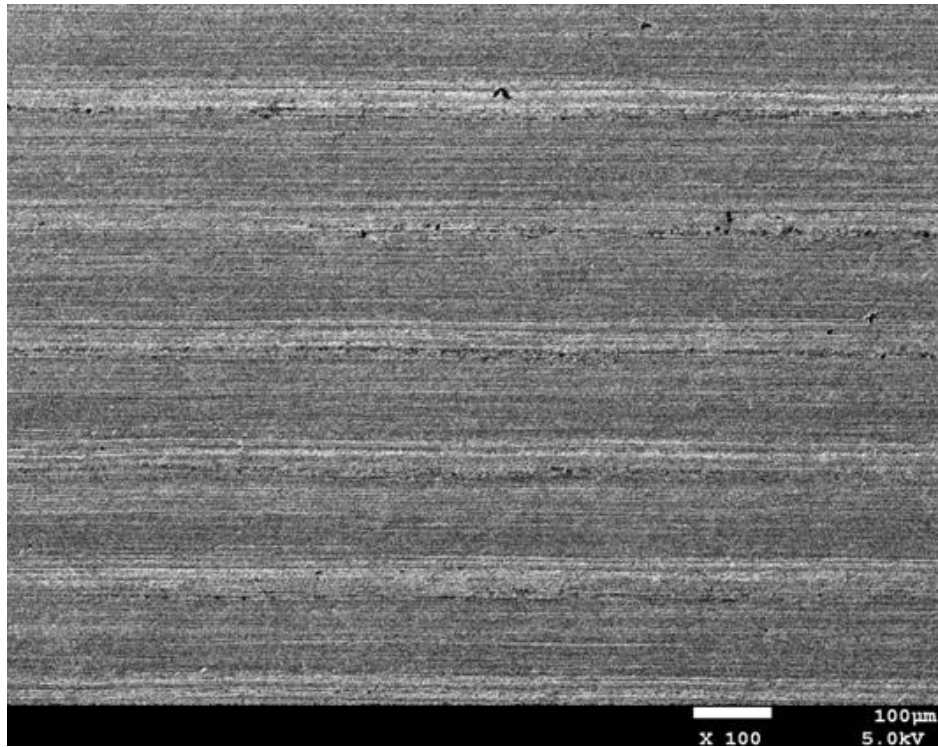
(a)
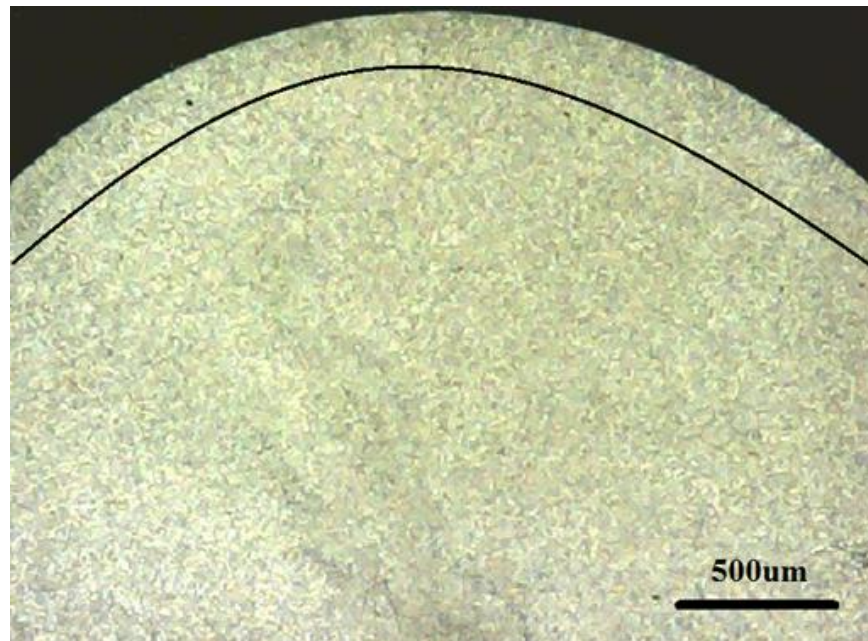
(b)

Fig. 4- (a) SEM image of surface of specimen after UNSM showing treatment marks (b) Cross-section of specimen after UNSM; the circular line shows the affected region of the cross-section having UNSM effect.
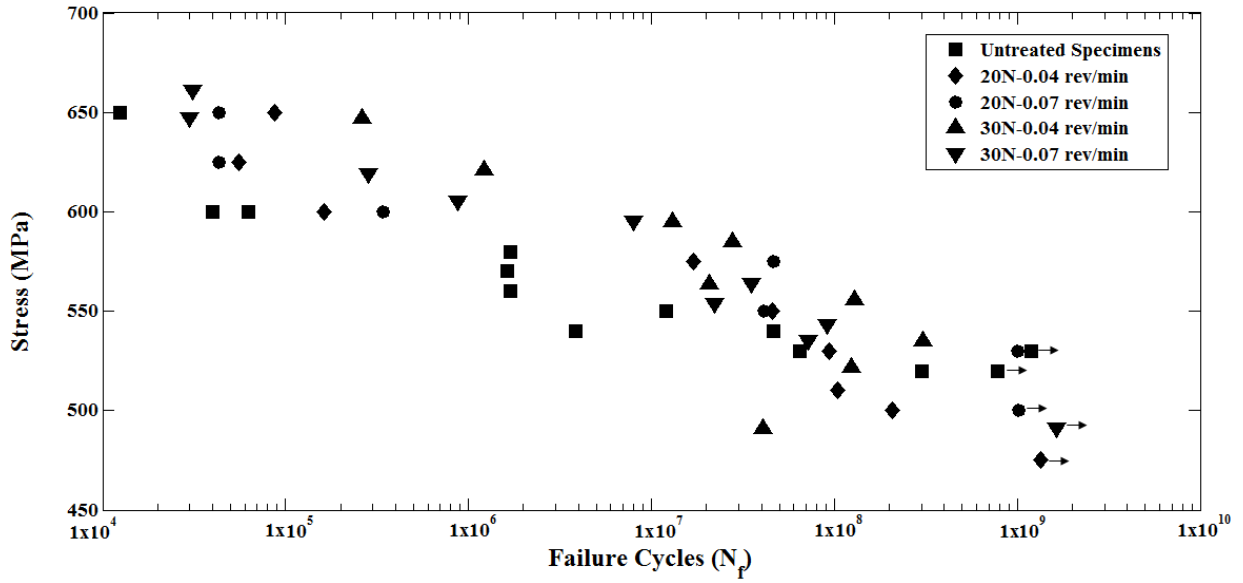
Fig. 5- S–N curve for AISI 310 stainless steel before and after UNSM treatment
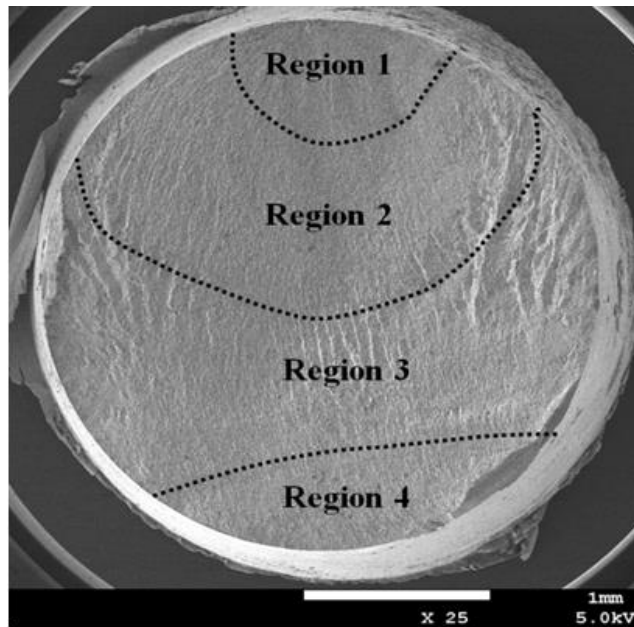
Fig. 6- Fracture surface of a specimen before UNSM treatment at 830MPa, 1.0605×10^5 cycles
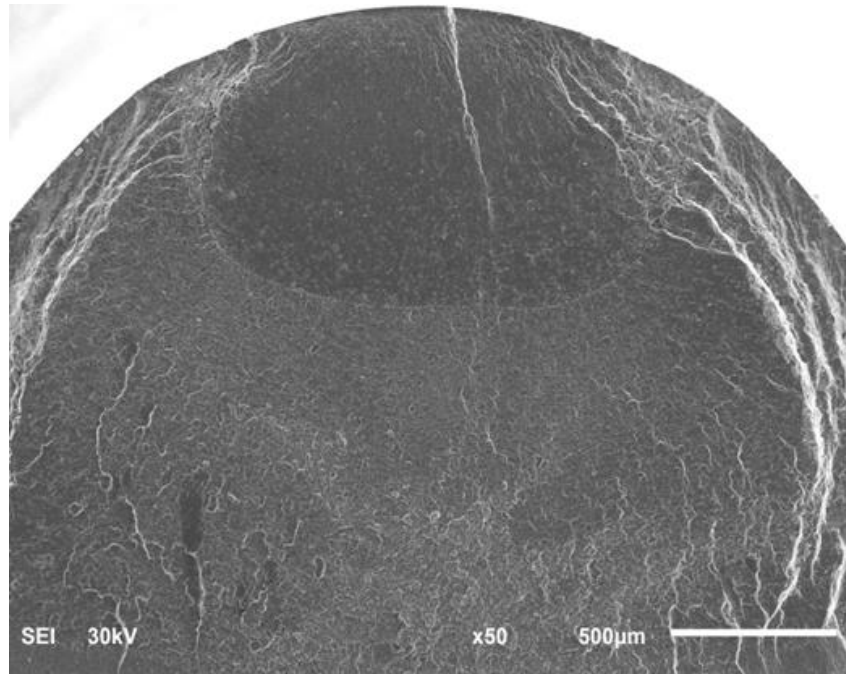
Fig. 7- Fracture surface of specimen treated with 20N impact force. The specimen was failed at 8.86×10^4 cycles and 650 MPa.
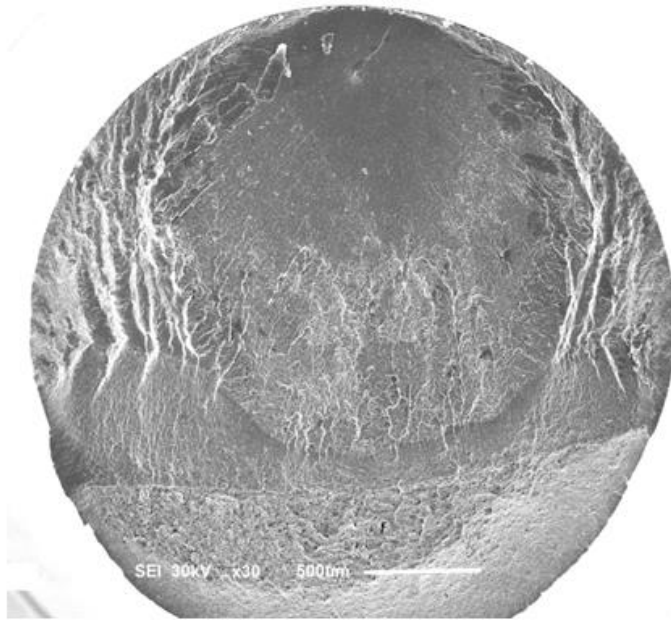
(a)
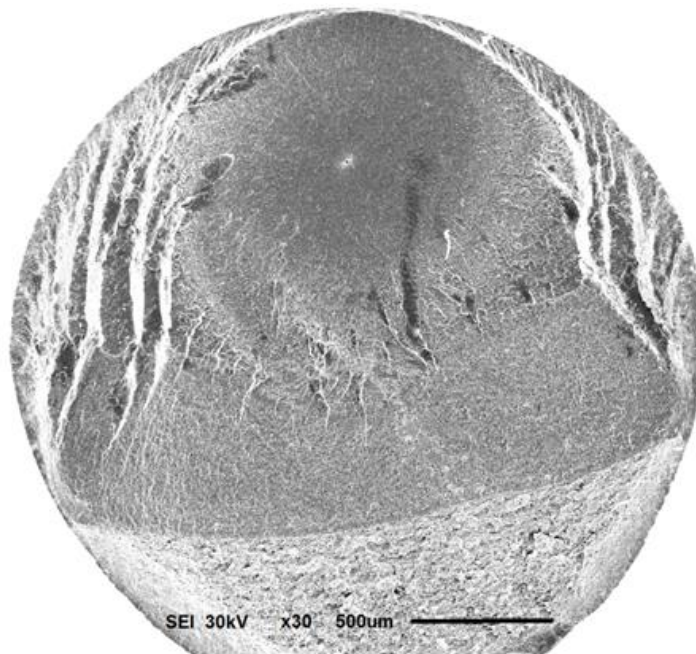
(b)

Fig. 8- Fracture surface of specimen after UNSM treatment at (a) 20N force and 0.04 rev/min feed rate failed at 4.6×10^7 cycles (b) 30N force and 0.07 rev/min feed rate at 3.069×10^8 cycles
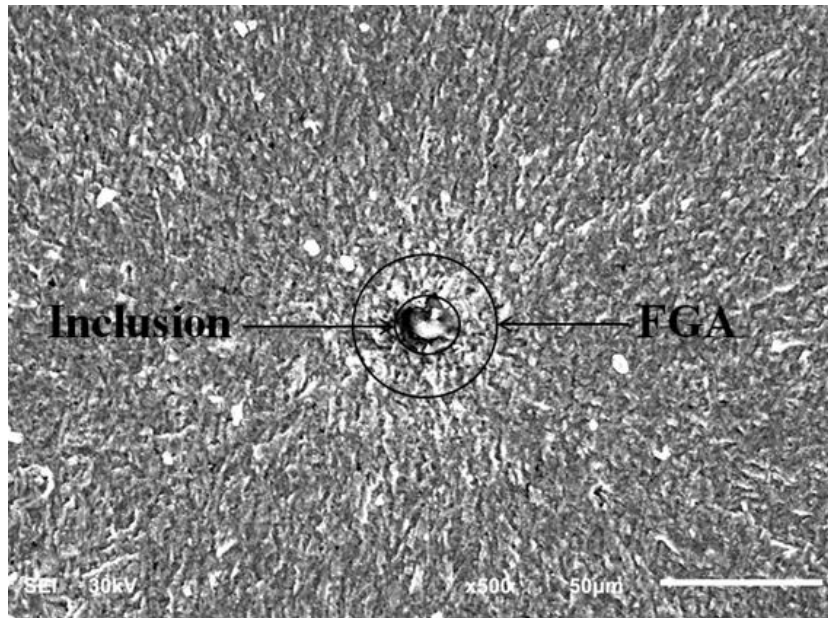
Fig. 9- Inclusion and FGA in a subsurface crack region
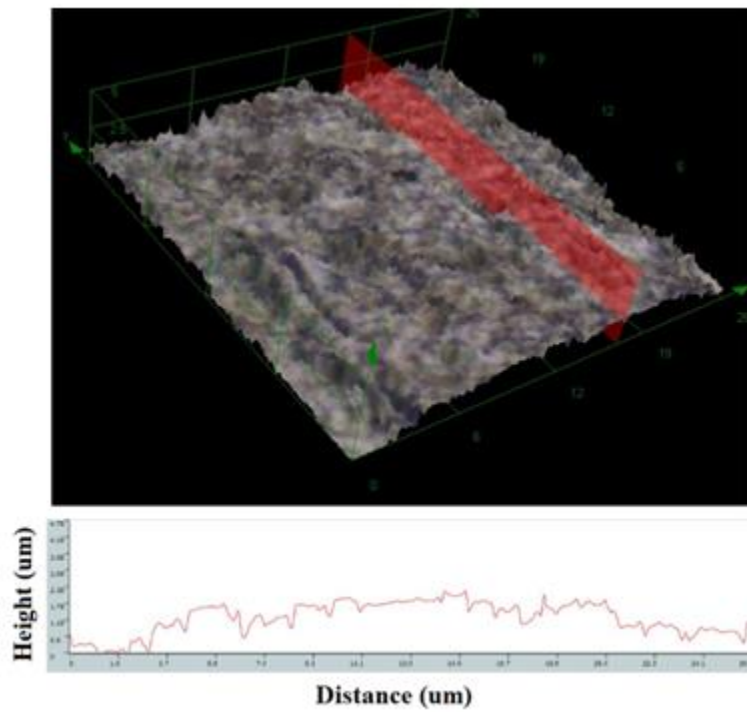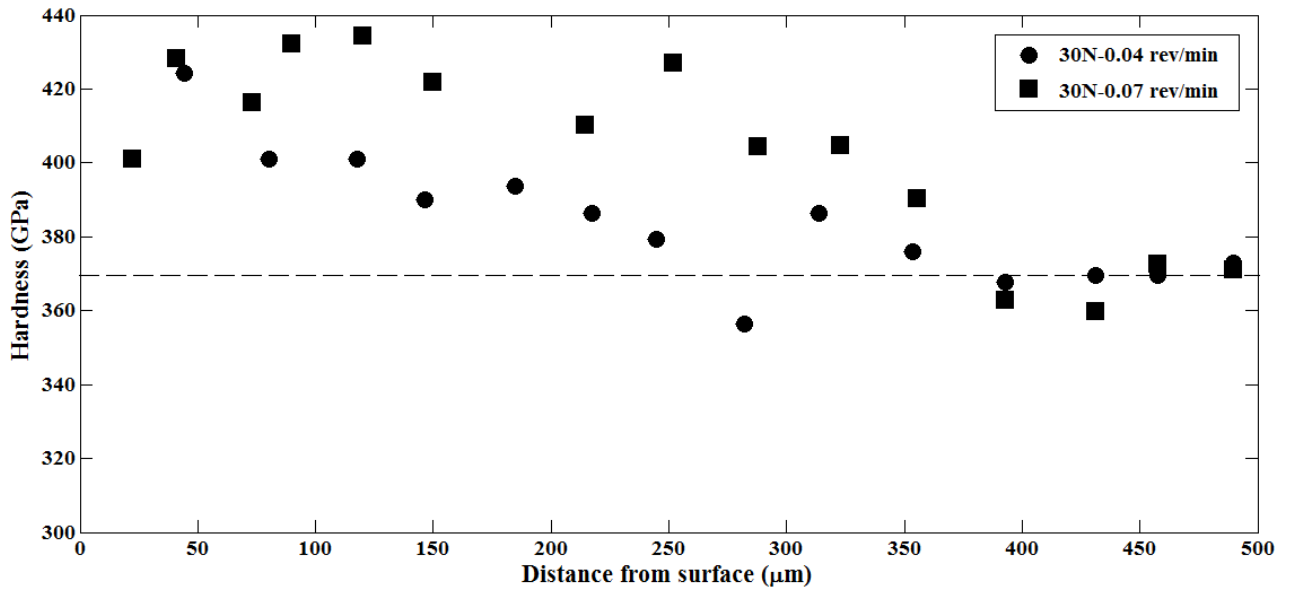

Fig. 10- Surface profile of a 25 μm x 25 μm region inside FGA
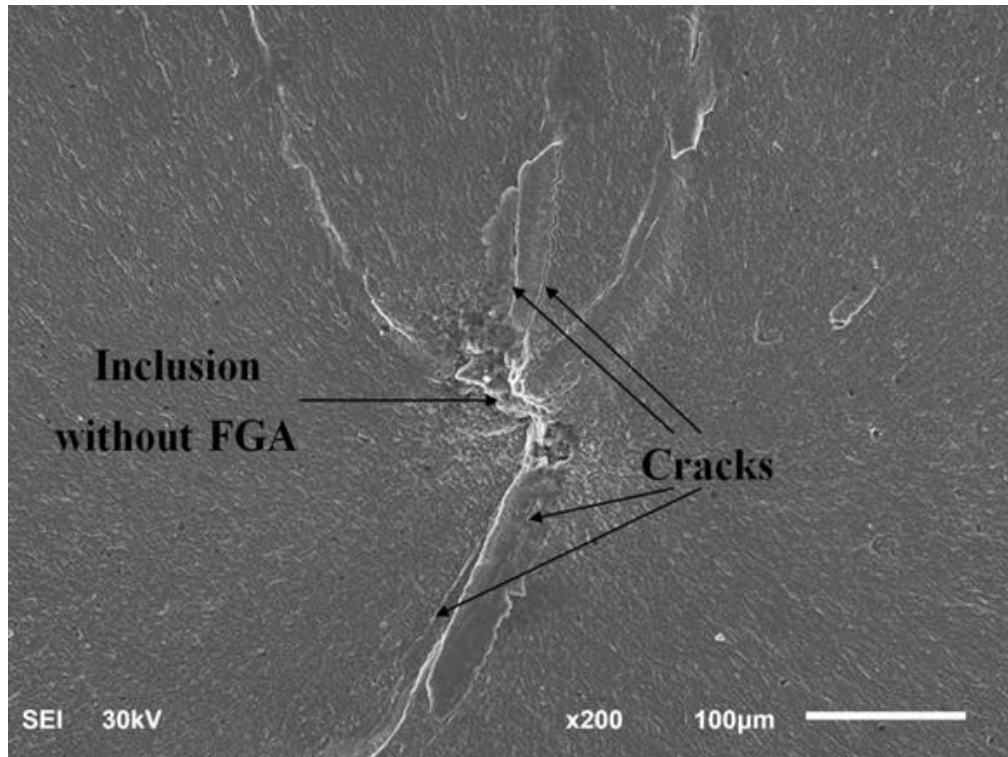
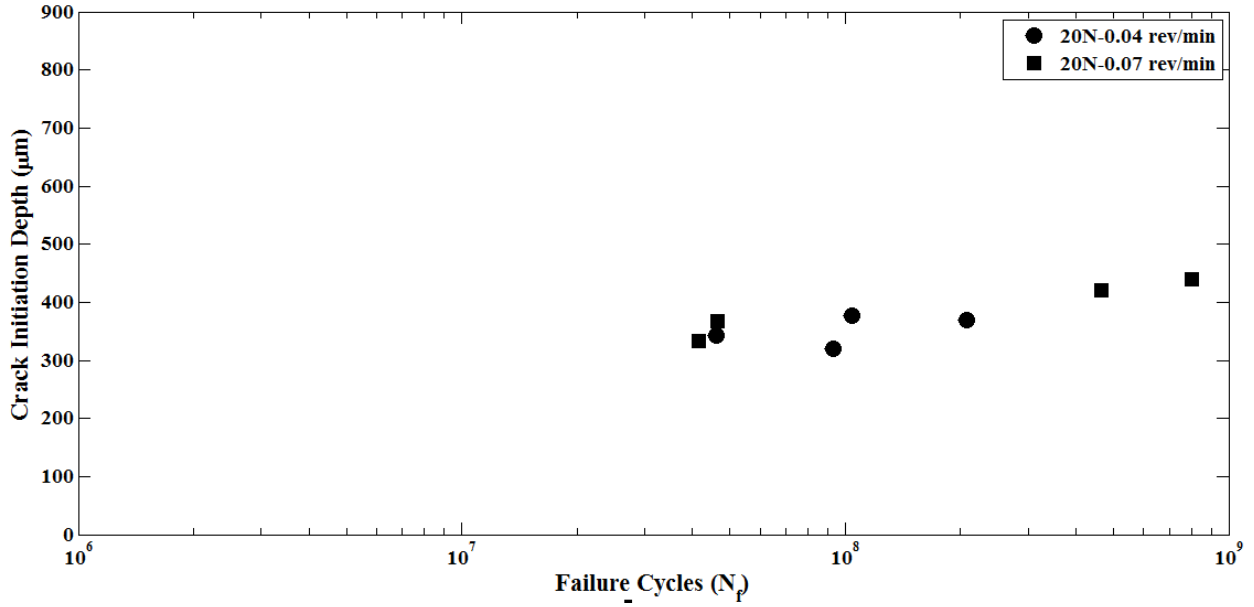**Fig. 11- Inclusion without FGA. Many cracks can be seen around the inclusion**
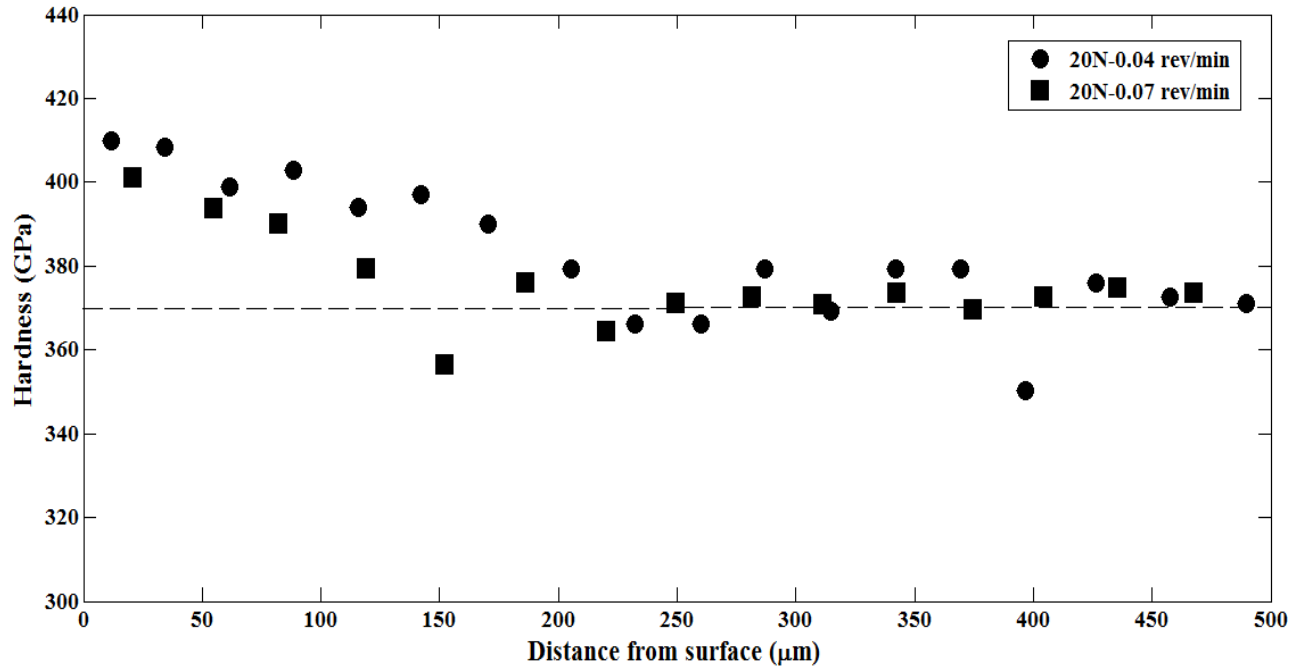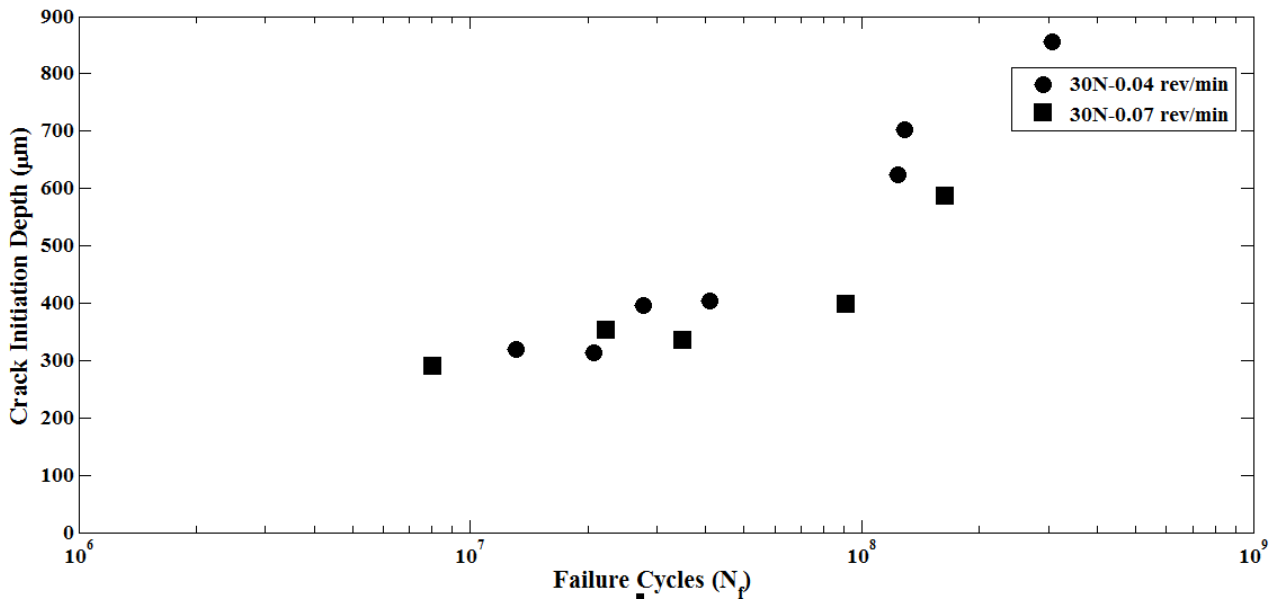
(a)

(b)

Fig. 12- Effect of surface treatment on the surface hardness with surface treatment force (a) 20N (b) 30N

(a)

(b)

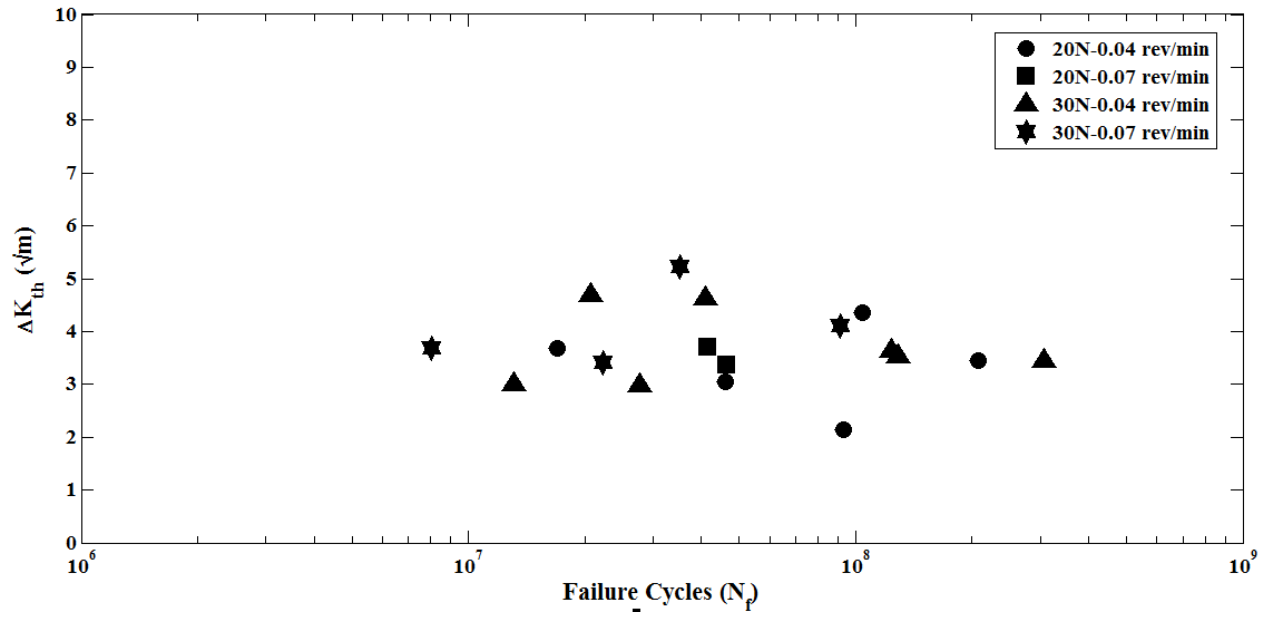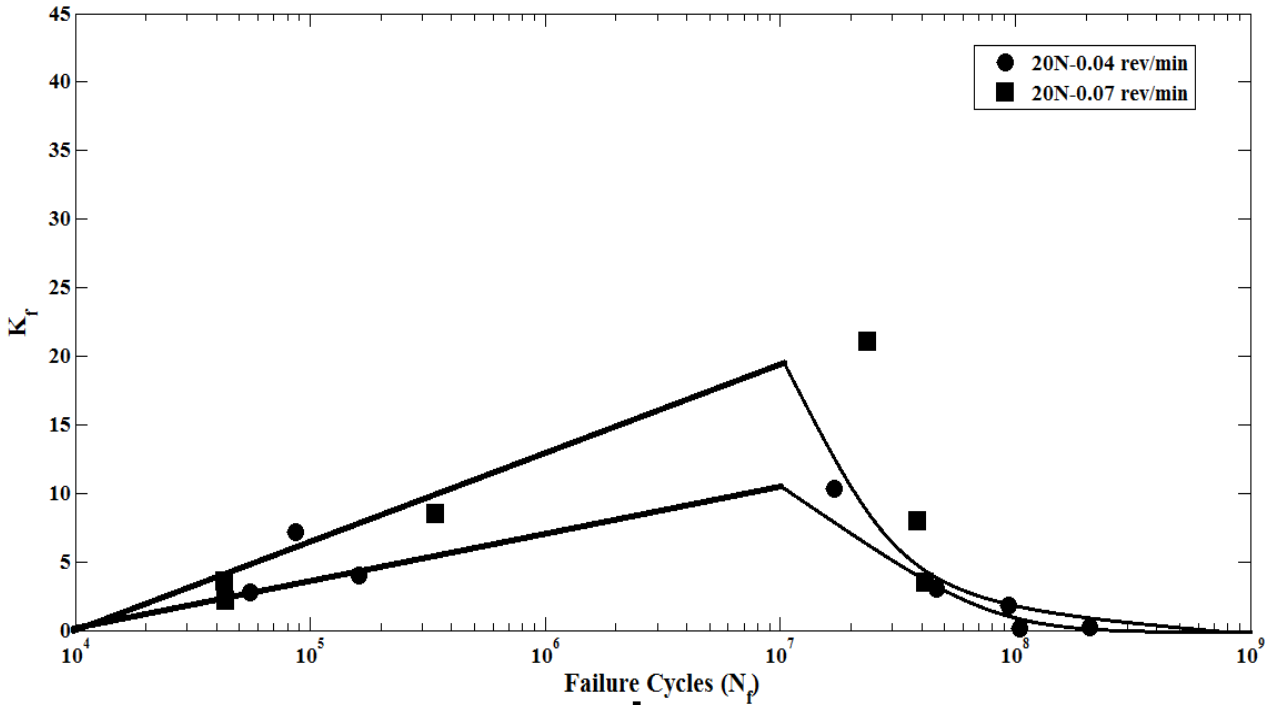**Fig. 13- Effect of surface treatment on the subsurface crack initiation depth after surface treatment force (a) 20N (b) 30N**
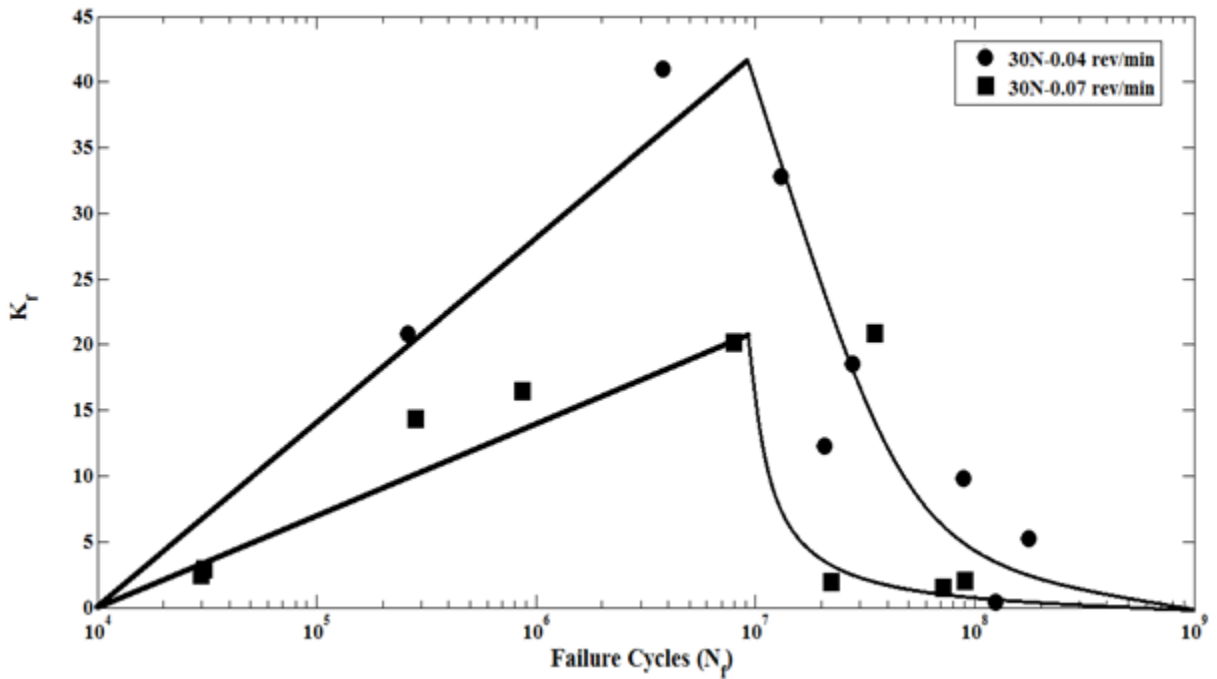
Fig. 14- Variation of ΔK_{th} in specimens shown subsurface cracking at different fatigue cycles

(a)

(b)

Fig. 15- Variation of K_f at different fatigue cycles in specimens treated with impact force of (a) 20N (b) 30N

Material	E (GPa)	σ_y (MPa)	Gauge length (mm)	Hardness (HV)	E / σ_y
AISI 310	205	850	25	370	240

Table 1- Mechanical property data for AISI 310

S. No	Specimen Type		Residual Stress (MPa)	
	Force (N)	Feed Rate (rev/min)	Longitudinal	Transverse
1	20	0.04	-280	-310
2	20	0.07	-295	-340
3	30	0.04	-360	-395
4	30	0.07	-375	-425

Table 2- Residual stress components on the surface of specimens treated with different UNSM parameters